



Disinfection by-product formation potential in response to variability in dissolved organic matter and nutrient inputs: Insights from a mesocosm study

Angela Pedregal-Montes^{a,b,*}, Eleanor Jennings^c, Dolly Kothawala^d, Kevin Jones^e, Johanna Sjöstedt^{e,f}, Silke Langenheder^d, Rafael Marcé^g, Maria José Farré^{a,b,*}

^a Catalan Institute for Water Research (ICRA), Carrer Emili Grahit 101, Parc Científic i Tecnològic de la Universitat de Girona, 17003 Girona, Spain

^b University of Girona, Plaça de Sant Domènec 3, 17004 Girona, Spain

^c Centre for Freshwater and Environmental Studies, Dundalk Institute of Technology, A91 K584 Dundalk, Ireland

^d Department of Ecology and Genetics/Limnology, Uppsala University, SE-75236 Uppsala, Sweden

^e Department of Biology, Aquatic Ecology, Lund University, Lund, Sweden

^f School of Business, Innovation and Sustainability, Halmstad University, Halmstad, Sweden

^g Centre for Advanced Studies of Blanes (CEAB), Spanish National Research Council (CSIC), 17300 Blanes, Spain

ARTICLE INFO

Keywords:

Climate change
Freshwater
Dissolved organic matter
Disinfection by-products
DBP formation potential
Mesocosms

ABSTRACT

Changes in rainfall patterns driven by climate change affect the transport of dissolved organic matter (DOM) and nutrients through runoff to freshwater systems. This presents challenges for drinking water providers. DOM, which is a heterogeneous mix of organic molecules, serves as a critical precursor for disinfection by-products (DBPs) which are associated with adverse health effects. Predicting DBP formation is complex due to changes in DOM concentration and composition in source waters, intensified by altered rainfall frequency and intensity. We employed a novel mesocosm approach to investigate the response of DBP precursors to variability in DOM composition and inorganic nutrients, such as nitrogen and phosphorus, export to lakes. Three distinct pulse event scenarios, mimicking extreme, intermittent, and continuous runoff were studied. Simultaneous experiments were conducted at two boreal lakes with distinct DOM composition, as reflected in their color (brown and clear lakes), and bromide content, using standardized methods. Results showed primarily site-specific changes in DBP precursors, some heavily influenced by runoff variability. Intermittent and daily pulse events in the clear-water mesocosms exhibited higher haloacetonitriles (HANs) formation potential linked to freshly produced protein-like DOM enhanced by light availability. In contrast, trihalomethanes (THMs), associated with humic-like DOM, showed no significant differences between pulse events in the brown-water mesocosms. Elevated bromide concentration in the clear mesocosms critically influenced THMs speciation and concentrations. These findings contribute to understanding how changing precipitation patterns impact the dynamics of DBP formation, thereby offering insights for monitoring the mobilization and alterations of DBP precursors within catchment areas and lake ecosystems.

1. Introduction

Rainfall events are fundamental for the transport of dissolved organic matter (DOM) and macro-nutrients such as nitrogen (N) and phosphorus (P) to the aquatic environment (Monteith et al., 2007). However, future climate scenarios, with increased warming and intensified precipitation patterns (Myhre et al., 2019), can alter DOM and nutrient export rates and may significantly affect the dynamics of

aquatic ecosystems and their services (Burd et al., 2018). Catchment characteristics play an important role in defining the composition of DOM and resulting water quality of freshwaters (Jennings et al., 2020). For example, an increase in terrestrial inputs of DOM to surface waters can lead to a decrease in water transparency in lakes, a phenomenon known as brownification (Weyhenmeyer et al., 2016). This effect has been observed in recent decades, particularly in the northern hemisphere (Anderson et al., 2023; Ledesma et al., 2012), and is linked to

* Corresponding authors.

E-mail addresses: apedregal@icra.cat (A. Pedregal-Montes), mjfarre@icra.cat (M.J. Farré).

<https://doi.org/10.1016/j.watres.2024.121791>

Received 5 March 2024; Received in revised form 10 May 2024; Accepted 14 May 2024

Available online 15 May 2024

0043-1354/© 2024 The Authors. Published by Elsevier Ltd. This is an open access article under the CC BY-NC-ND license (<http://creativecommons.org/licenses/by-nc-nd/4.0/>).

changes in land cover and uses, as well as climate change (Clutterbuck and Yallop, 2010).

Increasing levels of DOM in surface water sources represent a challenge for drinking water providers (Delpa et al., 2009; Lipczynska-Kochany, 2018). DOM is a main source of precursors for the formation of disinfection by-products (DBPs) during water disinfection processes in treatment plants (Dejaeger et al., 2022; Tak and Vellanki, 2018). These DBPs form when DOM reacts with chemical disinfectants added to water to destroy pathogens, posing health risks in drinking water (Evlampidou et al., 2020; Li and Mitch, 2018). Additionally, the presence of bromide and iodide ions in source waters can influence DBP speciation, leading to the formation of more toxic brominated and iodinated DBPs compared to their chlorinated analogs (Richardson, 2003). The identification of more than 700 DBP species reflects the impact of diverse DBP precursors and disinfection methods (Richardson, 2011; Wawryk et al., 2021). Nevertheless, current drinking water regulations primarily cover the better-characterized carbonaceous DBPs (C-DBPs), such as trihalomethanes (THMs) and haloacetic acids (HAAs), as well as chlorite, chlorate and bromate (Directive (EU), 2020/2184). However, some studies suggest that haloacetonitriles (HANs), a commonly occurring unregulated group of nitrogenous DBPs (N-DBPs), exhibit higher toxicity (Komaki and Ibuki, 2022; Wei et al., 2020).

Consequently, a promising strategy to surpass mere compliance with drinking water guidelines involves an enhanced understanding and monitoring of DBP precursors to i) improve their removal before disinfection and ii) predict DBP formation potential (DBP-FP) (Williams et al., 2019; Yang et al., 2008), a valuable surrogate for measuring the precursors in source water. Such a strategy is challenging, however, with DOM being one of the most complex and heterogeneous chemical mixtures in the environment (Leenheer and Croué, 2003).

Several properties of DOM have been linked to DBP-FP (Peleato and Andrews, 2015). The monitoring of DOM is often measured as bulk concentration, measured as either total organic carbon (TOC) or dissolved organic carbon (DOC) (Peng et al., 2016). Additionally, various methods have been developed to characterize the molecular composition of DOM. These range from simple optical techniques, such as ultraviolet (UV) absorbance and specific ultraviolet absorbance (SUVA) (Hua et al., 2015), to more sophisticated molecular-level mass spectrometry methods (e.g. Orbitrap-MS, FTICR-MS) (Farré et al., 2019). However, fluorescence spectroscopy is particularly advantageous as it is an accessible method for distinguishing DOM sources and tracking composition changes over time and space (Fellman et al., 2010). It provides insights into the presence of humic-like compounds associated with terrestrially-derived DOM and protein-like compounds associated with DOM from algae and bacterial sources in the aquatic environment (Fellman et al., 2010). The humic-like allochthonous DOM is strongly linked with the formation of C-DBPs, observations that are well documented (Golea et al., 2017; Wang et al., 2017). In contrast, protein-like autochthonous DOM has been associated with the formation of both C-DBPs and less understood N-DBPs (Wang et al., 2021).

While research on DBP formation is increasing in response to climate change impacts (Wang et al., 2022), the focus has predominantly centered on long-term mean environmental conditions. Meanwhile, the properties of stochastic events, such as rainfall intensity and frequency, which may have a more profound impact on freshwater quality, remain poorly understood (Jentsch et al., 2007). The monitoring of DBP precursors after rainfall events has been conducted at the intake of water

treatment plants (Delpa and Rodriguez, 2016; Xu et al., 2020) or through laboratory experiments simulating allochthonous DOM runoff (Chang et al., 2020). However, the impact of rainfall patterns on DBP precursors with autochthonous origins has received limited attention (Chen et al., 2008). Lastly, relevant relationships between DBP drivers and formation have been identified in the literature (Valdivia-Garcia et al., 2019), but they have primarily aimed at aiding water treatment decision-making rather than monitoring and controlling the mobilization of DBP precursors in source waters from catchments and lakes.

The overarching aim of this research was to investigate the response of DBP-FP to variability in the export of both DOM and nutrients to lakes, using a mesocosm approach. Mesocosms are field-based controlled studies that account for some of the complexity associated with processes occurring in the natural environment, while also allowing testing the effects of specific treatments (Boyle and Fairchild, 1997). While mesocosms are increasingly being used to study aquatic systems (Stewart et al., 2013), this is the first report, to our knowledge, of their use to investigate DBP precursors. The experimental design included both regional factors (e.g. replicating differing patterns in DOM pulses) and local factors (e.g. lake types). The experiment was conducted in two lakes in Sweden, each characterized by distinct ambient conditions: one with brown water and the other with clear water, yet both with similar DOC concentrations. Standardized equipment and methods were employed at both sites to investigate variations in DBP-FP levels and speciation for both regulated (THMs) and unregulated (HANs) DBPs. The study focused on three distinct patterns in pulse event scenarios involving additions of organic carbon (as DOC) and inorganic nutrients (as P and N) to the mesocosms, simulating runoff events. The three scenarios were simulated by manipulating the intensity and frequency of the additions to mimic extreme, intermittent, and continuous (daily) runoff conditions.

2. Methods and materials

2.1. Study sites and mesocosm facility

A spatially coordinated mesocosm experiment was conducted in two lakes to study the impact of runoff variability on DBP precursors in two different freshwater environments using the SITES AquaNet infrastructure (Urrutia-Cordero et al., 2021). Bolmen (56.9418 N, 13.6409 E) located in southern Sweden, is characterized as an oligotrophic humic lake with a mean depth value of 5 m. The second lake, Erken (59.835 N, 18.632 E) which is located in eastern Sweden, has a mesotrophic clearwater trophic status with a mean depth of 9 m. Both study sites have a hemiboreal climate with warm summers, the season during which this study took place (from July 7 to August 12, 2022). Table 1 presents the characteristics of the two water lakes. Despite similar DOC concentrations in both lakes, water from Bolmen has a high humic content (SUVA>4) while Erken water contains a lower level of humic substances with a mean SUVA value of 2 L mg⁻¹ m⁻¹.

A total of 16 high-density polyethylene cylindrical mesocosms (1.5 m height, 0.8 m diameter, 700 L total volume) were installed and fixed to a floating platform in each lake. Each mesocosm was filled by pumping 550 L of natural lake water from a depth of approximately 0.5 m below the surface to ensure the collection of a representative sample. The mesocosms in Bolmen will be referred to as 'brown mesocosm' hereafter, while those in Erken will be termed the 'clear mesocosm'. All mesocosms

Table 1
Lake water characteristics.

Lake	Mesocosm type	DOC (mg L ⁻¹)	A254 (cm ⁻¹)	SUVA (L mg ⁻¹ m ⁻¹)	Br* (μg L ⁻¹)	pH
Bolmen	Brown	10.4(0.58)	0.45(0.003)	4.34(0.29)	17(1.92)	7.01(0.22)
Erken	Clear	10.8(0.21)	0.22(0.001)	2.01(0.04)	120(5.19)	8.35(0.01)

Mean (SD) values (n=16) at Day 0.

* Mean (SD) historical values (2022) (n_{Bolmen}=10, n_{Erken}=27).

featured closed bottoms and open tops, strategically positioned to float within the lake waters, maintaining a natural and ambient temperature regime. Additional protocols about the experiment setup are available in [Langenheder et al., 2024](#).

2.2. Experimental design

Runoff variability was experimentally simulated by manipulating the frequency and intensity of natural DOM and nutrient loading regimes to the mesocosms, with pulses of DOC in the form of peat extract solution, as well as pulses of inorganic nutrients (N as NaNO_3 and P as KH_2PO_4). Each mesocosm received the same total amount of DOC and inorganic nutrients, but these additions were supplied at three different intervals or treatments: extreme (E), intermittent (I), and daily (D) (Figure A.1). Overall, each treatment (E, I, D) received a total addition of 2 mg L^{-1} of DOC, $500 \mu\text{g L}^{-1}$ of N, and $50 \mu\text{g L}^{-1}$ of P.

Consequently, the experimental setup comprised: (1) the extreme treatment, where mesocosms received a low-frequency but high-intensity pulse event scenario (one addition, 100 % total addition) on Day 7, (2) the intermittent treatment, which received a medium frequency and medium-intensity pulse event scenario (seven additions ranging from 5 % to 30 % of total addition), and (3) the Daily treatment, consisting of a high frequency but low-intensity pulse event scenario (20 additions of 5 % of total addition each) starting from Day 0 to Day 19. In addition, a reference treatment, the unmanipulated control (C), with no additions, was incorporated in the experiment.

The experiment lasted for a total of 37 days, mimicking a rainfall period (the additions period). This period included the first 20 days during which the additions occurred, followed by a subsequent 17-day recovery period with no further additions (Figure A.1) to determine whether the effects of pulse manipulation persisted. While a rainfall event can contribute to a dilution effect ([Chang et al., 2020](#)), here we considered a significant positive relationship between DOC and runoff, as observed in other streams draining wetlands ([Kothawala et al., 2015](#)), especially during the summer when decomposition in catchment soils is highest ([Jennings et al., 2020](#)).

All treatments, including the control, were replicated four times, and each treatment was randomly assigned to one of the four pools of the floating platform ([Langenheder et al., 2024](#)). The mesocosms were filled on 6 July 2022 (Day -1), and the first samples representing the initial conditions (before additions) were collected on 7 July 2022 (Day 0).

2.3. Peat extract and nutrient preparations

For the addition of DOC, a solution of natural DOM was extracted through alkaline extraction ([Riedel et al., 2012](#)) from commercially available peat (Hasselfors Solmull Naturtorv®) as described in [Langenheder et al., 2024](#). The preference for peat leachate over commercially available extracts, such as HuminFeed® was based on the highly recalcitrant characteristics of these other reference materials ([Calderó-Pascual et al., 2021](#)). Solutions of NaNO_3 and KH_2PO_4 were prepared to adjust the target total nutrient additions of $500 \mu\text{g L}^{-1}$ of N and $50 \mu\text{g L}^{-1}$ of P, respectively ([Langenheder et al., 2024](#)). The DOC solution from the peat extract and the concentrated inorganic nutrient solutions were stored frozen in batches (falcon tubes previously autoclaved) in accordance with the target addition for each treatment and replicate. The required batches (see Section 2.2) were removed from the freezer the day before the addition and allowed to thaw overnight.

2.4. Mesocosm water monitoring strategy

Water temperature (T_w) and dissolved oxygen concentration (DO) (Optode, Aanderaa Data Instruments AS) were recorded continuously using sensors installed in each mesocosm at a depth of 0.6 m ([Urrutia-Cordero et al., 2021](#)). An underwater photosynthetically active radiation (PAR_U) sensor was installed at a depth of 0.4 m in each

mesocosm. A handheld multiprobe system (EXO2, YSI) was used to measure pH at 0.6 m depth in each mesocosm daily. More information regarding sensors handling and data treatment is available in ([Langenheder et al., 2024](#)). Meteorological data, air temperature ($^{\circ}\text{C}$) and total precipitation (mm day^{-1}), were collected from the local weather stations [Erken Laboratory, 2023](#).

On sampling days, an integrated water column sample was collected using a Ruttner sampler. Samples were transported to the laboratory immediately and subsampled into different aliquots for total dissolved nitrogen (DN), total phosphorus (TP), chlorophyll-a (Chl-a), UV absorbance at 254 (A254) and 420 (A420) nm, and DOC analysis. The unused surplus water sample was returned to its respective mesocosm.

Samples for DOC, nutrients and Chl-a were analyzed six times (on Days 0, 4, 8, 12, 20 and 36) following methods described in ([Langenheder et al., 2024](#)). The UV absorbance of water samples was measured every four days using a HACH DR6000 and Shimadzu UV-1800 spectrophotometer for samples from brown and clear mesocosms, respectively. Quartz cuvettes of 5 cm were used for measuring A420 to characterize water color as a brownification proxy ([Weyhenmeyer et al., 2016](#)), while cuvettes of 1 cm were employed for measuring A254. The A254 values were used to calculate SUVA values, serving as a surrogate for aromatic and humic DOM ([Hua et al., 2015](#)).

2.5. DOM composition

Samples for fluorescence spectroscopy measurement of DOM were collected at six time points (Days 0, 4, 8, 12, 20 and 36) directly from the Ruttner sampler and transferred to acid-washed plastic tubes at the mesocosm platform. Samples were filtered through pre-rinsed PES-syringes filters ($0.2 \mu\text{m}$ pore size) and stored in acid-washed pre-combusted glass vials at 4°C in the dark. One sample blank (using Milli-Q water) was included per sampling day and underwent the same process as mesocosms water samples to check for possible contamination. Both absorbance and fluorescence excitation emission matrices (EEM) were simultaneously measured using a Horiba AquaLog® fluorescence spectrophotometer using a 1 cm quartz cuvette and Milli-Q water to blank correct and define the baseline. Fluorescence was measured for all samples from brown and clear mesocosms within 8 days after the experiment. The excitation wavelengths spanned from 240 to 600 nm (3 nm increments), while emission wavelengths ranged from 246 to 827 (4.65 nm increments), and the integration time was 0.5 s. Spectral corrections were performed by AquaLog®, while inner filter effects were corrected by drEEM toolbox ([Murphy et al., 2013](#)) in MATLAB® (R2022b) using the corresponding absorbance measurements ([Kothawala et al., 2013](#)). All EEMs were analyzed and processed using the drEEM toolbox. Fluorescence intensities were normalized to Raman Units (RU) ([Lawaetz and Stedmon, 2009](#)) and EEMs were resized to commonly used ranges (excitation: 250–500; emission: 300–600 nm) since no reliable fluorescence was detected outside the ranges. After removing Raman and Rayleigh scatters, outliers were identified and removed using built-in functions.

A multi-variate tool used to identify underlying fluorescence components, parallel factor (PARAFAC) analysis was applied to the pre-processed EEMs following the iterative steps provided by [Murphy et al., 2013](#). After internal (Split-half analysis) model validation, the PARAFAC components were compared with OpenFluor database, finding matches for all the components (similarity score > 0.95) ([Murphy et al., 2014](#)). The optimal PARAFAC model capable of describing the DOM pool within the dataset revealed six fluorescence components (Table A.1). Notably, three PARAFAC components exhibited multiple excitation loadings, and all emission loadings displayed smooth uni-modal peaks, consistent with expectations for fluorophores ([Stedmon and Bro, 2008](#)). Four components (C1, C2, C3, C4) demonstrated spectra resembling humic-like peaks, while two components (C5, C6) exhibited spectra akin to protein-like peaks. Additionally, the relative fluorescence intensity was calculated and expressed as a percentage to

assess changes in DOM composition during the experiment.

2.6. DBP-FP tests

Water samples were collected four times (Days 0, 8, 20 and 36, all days that overlapped with sampling for DOM, nutrients, and Chl-a) and immediately stored frozen in the dark until DBP-FP tests were performed. The DBP-FP was conducted following methods of previous studies (Liu et al., 2016; Munthali et al., 2022; Sanchís et al., 2020) to obtain between 1 and 3 mg L⁻¹ of residual free chlorine after 4 days of contact time to allow the reaction to approach completion for all the samples (APHA, 2005; Uzun et al., 2020). The determined chlorine dose was added to all samples, prior to incubating in head-space free glass tubes in the dark at 22 °C. The samples were quenched with ascorbic acid after measuring their residual chlorine content (LCK 310, Hach Lange GmbH, Germany).

Samples were liquid-liquid salt extracted (in duplicate) with Methyl-t-Butyl Ether (MtBE) at a pH of 3.5 and analyzed by gas chromatography coupled to mass spectroscopy (GC-MS) (Thermo Fisher Scientific). Further details about the GC/MS method are available in Munthali et al., 2022; Sanchís et al., 2020. The identified DBP species were categorized into two groups: (1) THMs, which included chloroform (TCM), bromodichloromethane (BDCM), dibromochloromethane (DBCM), and bromoform (TBM), constituting part of the C-DBPs; and (2) HANs, including dichloroacetonitrile (DCAN), trichloroacetonitrile (TCAN), bromochloroacetonitrile (BCAN), and dibromoacetonitrile (DBAN), forming part of the N-DBPs. While additional C-DBPs such as 1,1-dichloropropane (1,1-DCP), 1,1,1-trichloropropane (1,1,1-TCP), and trichloronitromethane were measured, only the last one was quantified at concentrations above the limit of detection. Consequently, our analysis focused on the THMs and HANs species.

2.7. Data analysis

All statistical analyses and graphs were conducted using R version 4.2.3. (R Core Team, 2023). Initial conditions (before additions) were compared between treatments (C, D, I, E) and mesocosm types (brown and clear) through a two-way ANOVA applying additive models on all variables at Day 0 (Fonseca et al., 2022). To assess statistical differences among treatments after the additions, pairwise comparisons (*t*-test) were performed for each sampling day (Day 4, 8, 12, 20 and 36) using treatment (C, D, I, E) as factor, for brown and clear mesocosms separately. The pairwise comparisons were applied separately for the different variables assuming that they were independent datasets from different samplings. The *t*_test function from the *rstatix* package was used, and *p*-values were adjusted using the Bonferroni method to account for the number of comparisons (Calderó-Pascual et al., 2021).

Non-metric multidimensional scaling (NMDS) was employed to compare the formation potential of DBPs between mesocosm types across the entire experiment using the *vegan* package. Given the expected diverse responses in DBP-FP and non-linear associations between variables, the robust ordination technique of NMDS was suitable for analyzing our dataset (Clarke, 1993). The dissimilarity matrix was constructed based on 125 observations, incorporating all DBP species quantified at concentrations above the limit of detection. The low stress value of 0.04 of the NMDS analysis indicated that the ordination effectively represented the high-dimensional assemblage structure. Subsequently, an ANOSIM post-analysis test was conducted to evaluate statistical dissimilarity. To assess the behavior of potential explanatory variables and their relationships with the formation of DBPs; nutrients, Chl-a, PARAFAC components intensities, SUVA, A420 and DOC, all referred to collectively as environmental variables, were fitted onto the NMDS ordination using the *envfit* function.

The effects of DOM and nutrient additions on DBP-FP for THMs and HANs were examined for brown and clear mesocosm types separately. Linear mixed effects (*lme*) models, implemented with the *nlme* R

package, were employed for the analysis (Feuchtmayr et al., 2019). Each model included a random intercept fitted for one random variable, mesocosm number (1 to 16), accounting for variations in DBP-FP. The models considered the day of experiment (0, 8, 20 and 36), treatments (C, D, I, E), and their interactions. Assumptions were verified by visually inspecting residuals for normality and constant variance.

Finally, partial least squares (PLS) models were employed to assess multicollinearity in the data set and to establish the relationships of the formation of DBPs (response variable) with the explanatory variables used previously in the NMDS analysis. Two PLS models were constructed, one for THM and another one for HAN formation potential for brown and clear mesocosm types. The determination of the number of PLS components was based on the test root mean squared error (RMSE) and validated through the leave-one-out cross-validation method. Variable Importance in Projection (VIP) was used to identify the most influential explanatory variables in the PLS models. The larger the VIP value, the more importance of an explanatory variable for the response variable. VIP values greater than one are considered to be the relatively important explanatory variables (Favilla et al., 2013). The necessary packages for this analysis included *pls*, *vip*, *caret* and *PROC*.

3. Results and discussion

3.1. Climate and initial conditions

During the study period, air temperature fluctuated from 6°C to 33°C for the brown mesocosms and from 10°C to 36°C for the clear mesocosms. Precipitation during the experiment was sporadic at both locations. Surface water temperature in the mesocosms generally tracked the changes in air temperature. Despite a broader spectrum of water temperatures observed in brown mesocosms, both the brown and clear mesocosms maintained a comparable mean temperature of 20°C throughout the experiment.

The differences in initial conditions of the experiment (before additions) were identified between the brown and clear mesocosm types through the application of a two-way ANOVA for Day 0. Significantly higher values of PAR_U, A420 and SUVA (*p* < 0.001) were observed in the brown mesocosms compared to the clear mesocosms, which are sensitive indicators of browning (Table A.2). Humic-like PARAFAC components (C1, C2, C3, C4) were higher in the brown mesocosms, while protein-like PARAFAC component C6 showed no significant differences between mesocosm types (*p* = 0.758), and C5 exhibited higher values in the clear mesocosms (*p* < 0.01) (Table A.2). Regarding the initial composition of DOM, both brown and clear mesocosms were predominantly composed of humic-like components, with 82 % and 69 %, respectively (*n* = 16) (Figure A.2). This composition was consistent with typical natural water as reported by (Eder et al., 2022). Less significant differences were observed for DOC, DN and Chl-a (*p* < 0.05), and no significant differences were observed for TP (*p* = 0.166), with lower mean concentrations of DOC (10.4; 10.8 mg L⁻¹), DN (472.1, 504.1 µg L⁻¹) and TP (19.5; 20.4 µg L⁻¹), and higher Chl-a values (5.84; 4.77 µg L⁻¹) for the brown mesocosms compared to the clear mesocosms (*n* = 4) (Table A.2).

The formation potential of HANs before the additions was not significantly different between the brown and clear mesocosms (*p* = 0.17) (Table A.2). However, significantly lower mean initial levels of THMs were found in the brown mesocosms (256.1 µg L⁻¹) compared to clear mesocosms (359.4 µg L⁻¹) (*n* = 4) (Table A.2), which contradicts the typical association of higher THMs formation in humic waters (Bond et al., 2012). In particular, high concentrations of bromine containing THMs were found in clear mesocosms (Table A.3) due to the higher concentration of bromide in those source waters (Table 1). Hypobromous acid (HOBr) is very rapidly formed by the reaction of Br⁻ and HOCl (*k* = 1.5 10³ M⁻¹s⁻¹) (Kumar and Margerum, 1987). In numerous instances, the reactivity of HOBr in halogenation reactions significantly surpasses that of HOCl (Criquet et al., 2015; Hua et al., 2006; Lee and

Von Gunten, 2009). For example, studies have demonstrated that the second-order rate constants for reactions involving phenolic compounds are, on average, 3000 times higher for HOBr in comparison to HOCl (Heeb et al., 2014). Therefore, the higher formation potential of THMs (mostly Br-THMs) was likely a function of the higher concentration of bromide observed in the clear waters in comparison to the brown waters.

3.2. DBP-FP across treatments and mesocosm types

The NMDS analysis shows a tight clustering of DBP-FP by mesocosm type, brown and clear, when all days of the experiment and all treatments were included (Fig. 1). The smaller tightly clustered ellipse for the brown mesocosms suggested a more uniform response over time and across treatments. This consistent and temporally stable response suggests that brown mesocosms were more resistant to changes induced by the pulse events, regardless of their frequency. In comparison, the larger ellipse for clear mesocosms reflects a greater dispersion of observations over time and treatment. This dispersion may indicate an elevated susceptibility of clear mesocosms to the treatments regarding alterations in DBP precursor concentrations. A post-analysis ANOSIM gave a test statistic of 0.973 ($p = 0.001$), indicating a highly significant dissimilarity between the DBP-FP data from the brown and clear mesocosms, respectively.

Potential explanatory variables were overlaid on the NMDS plot as environmental vectors (Fig. 1). The direction and length of arrows for humic-like components (C1, C2, C3, C4), SUVA and A420 suggested correlations with DBP-FP in brown mesocosms. In turn, protein-like components (C5, C6), DN and DOC exhibited correlations with DBP-FP in the clear mesocosms. Further analysis of these correlations was explored in Section 3.5.

These results collectively indicate that the DBP precursors present in the water of each respective mesocosm type and/or the prevailing environmental conditions at the individual study site exerted a dominant role in the process of DBP formation potential within the scope of this investigation. Given the significant dissimilarity identified between brown and clear mesocosms, we proceeded with data analysis for each mesocosm type separately.

3.3. Impact of DOM and nutrients additions on DBP precursors

The additions of DOM and nutrients affected the DBP precursors of the brown and clear mesocosms differently. Brown mesocosms, rich in background levels of humic substances, tended to manifest a comparatively lower response to the three distinct pulse additions (D, I, E). Interestingly, the stable DOM composition in brown mesocosms throughout the experiment (Figure A.2) aligned with the observed low biological activity from phytoplankton, as indicated by trends in DO, pH, and Chl-a (Figures A.3 and A.4) (Lavonen, 2015). Only a minor increase of approximately 1 % in protein-like components was observed within the ecosystems for brown waters at the end of the experiment (Day 36) (Fig. A.2). Pilla and Griffiths, 2023 conducted a study on the “hump-shaped” relationship between Chl-a and DOC concentrations, suggesting that increases in DOM-bound nutrients stimulate primary production (with Chl-a as a proxy) until light availability becomes a limiting factor for growth. This observation aligns with several studies, generally performed in boreal lakes, which emphasize that in some cases colored terrestrial organic matter can have a more dominant control in limiting productivity than nutrients (Lavonen, 2015; Soulié et al., 2022).

A more detailed examination of the temporal dynamics of the six PARAFAC components was conducted using time series data for maximum fluorescence (Fmax) (Fig. 2). In brown mesocosms, humic-like components of DOM showed patterns similar to A420 and SUVA (Fig. A.3), showing positive responses to the pulses during the additions period and clustering together from Day 20 onwards. Despite components C2 and C4 exhibited decreasing trends during the recovery period (Figs. 1-c and 1-g), significantly higher Fmax values were observed for all PARAFAC components except C5 at Day 36 for all three treatments with respect to the control mesocosms (Fig. 2, Table A.4). This suggests that the impact of all pulse treatments in the brown mesocosms persisted even after the recovery period. The poor response of the brown mesocosms to the different pulses in this study is consistent with the observations of previous studies (Karlsson et al., 2009).

Contrarily, the clear mesocosms exhibited heightened sensitivity to the pulses. The protein-like components increased in the clear mesocosms across the experiment for all treatments (Figure A.2). These components have been related to autochthonous freshly produced DOM (Coble et al., 1990; Parlanti et al., 2000), where humic-like proportions decreased with increasing water residence time (Fig. A.2), indicating

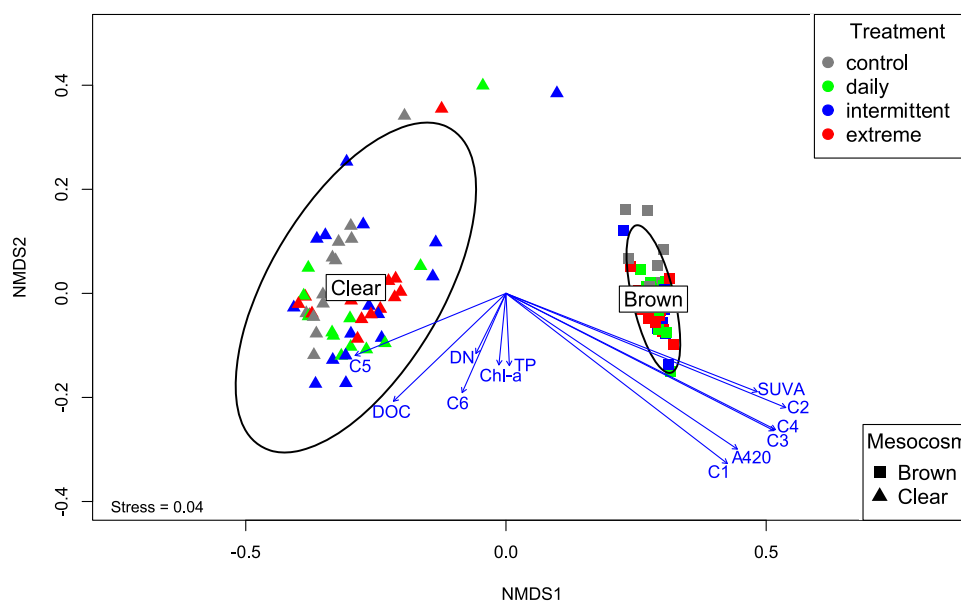


Fig. 1. NMDS plot based on concentration of quantified DBP-FP species (TCM, BDCM, DBCM, DCAN, TCAN, BCAN) from both brown and clear mesocosms across all sampling days ($n = 113$). Arrows represent the relationship between potential explanatory variables and DBP-FP. Ellipses are shown with a 95 % confidence level and show the dispersion of the observations grouping by mesocosm type.

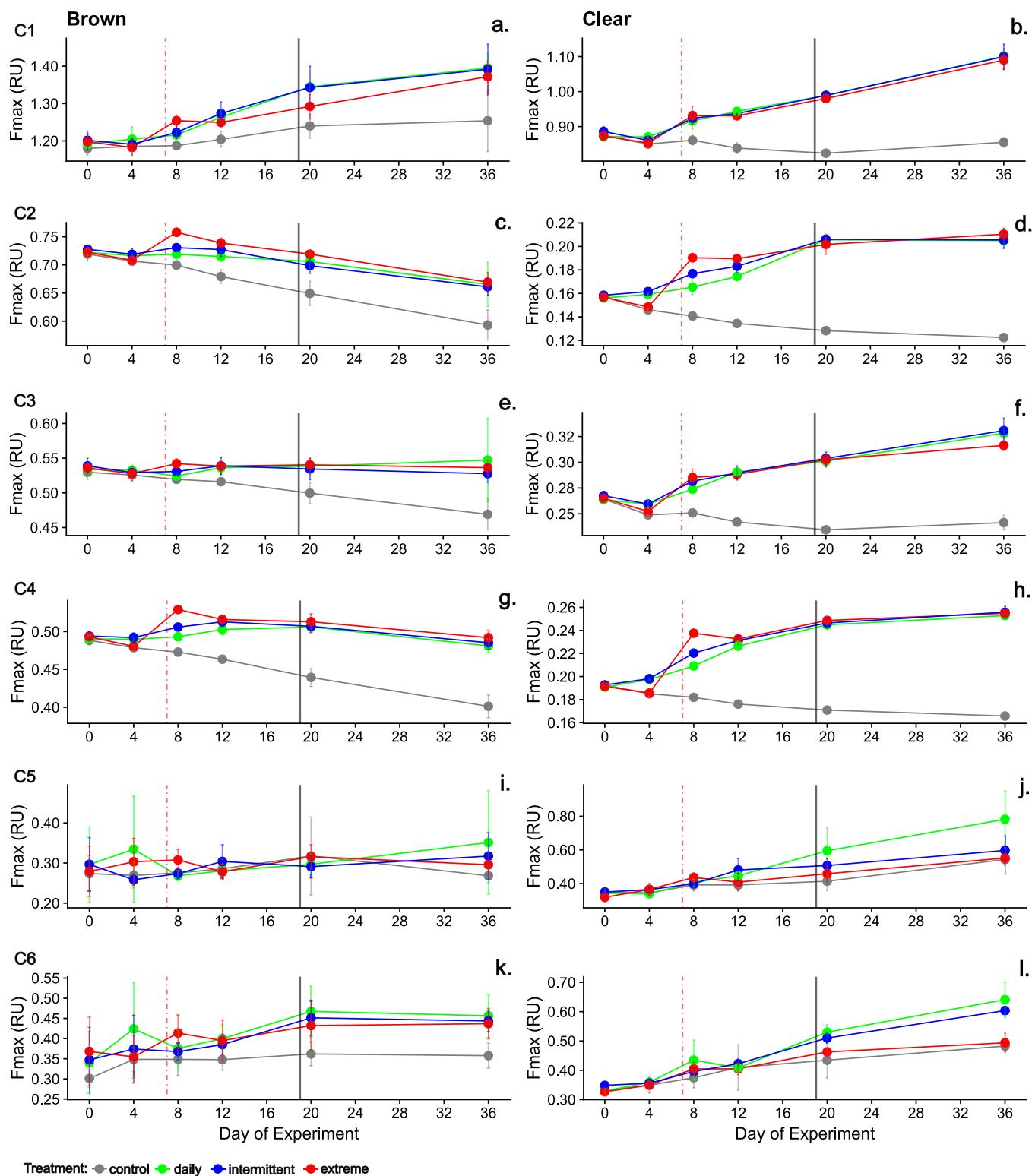


Fig. 2. Changes over time in the six PARAFAC components using maximum fluorescence (F_{max}) (mean \pm sd, $n = 4$). Red vertical dashed lines indicate when the extreme pulse took place. Gray vertical lines indicate the end of the additions period.

shifts in DOM composition (Bertilsson and Tranvik, 2000; Kothawala et al., 2014). These observations aligned with the A420 and SUVA trends that exhibited a decline during the recovery period (Day 20 to Day 36) (Figs. A.3-f and A.3-h; Table A.4), suggesting DOM transformations in the water. F_{max} time series for the clear mesocosms exhibited significantly higher values of the protein-like components C5 and C6 for daily and intermittent treatments after the additions period and showed

positive trends until the last day (Figs. 2-j, 2-i; Table A.4). These results suggest that there was sufficient light penetration for algae growth in the clear mesocosms, and that the frequency and intensity of daily and intermittent nutrient pulses may have enhanced higher biological activity in these waters as shown in the DO, pH and Chl-a trends (Fig. A.3) (Feuchtmayr et al., 2019). Additionally, fresh DOM produced within lakes has higher nitrogen content (Hua et al., 2019; Leenheer, 2009),

which was observed in the temporal series of DN for the clear mesocosms (Figure A.3-j).

3.4. Response of DBP-FP to pulse additions

The formation potential of THMs was lower in brown mesocosms throughout the experiment (Fig. 3-b, Table A.3). Despite observing increases in THMs after the different additions, the results from the lme model showed that the total THM-FP in brown mesocosms was not significantly impacted by the different pulse additions throughout the experiment (Fig. 3-a, Table A.6). Additionally, the THMs speciation found at Day 0 remained almost constant after the additions, with average TCM and BDCM concentrations of $240 \mu\text{g L}^{-1}$ and $12.3 \mu\text{g L}^{-1}$, respectively ($n = 48$, Day>0) (Fig. 3-b). In contrast, the presence of elevated bromide in clear mesocosms increased the formation of THM species, with elevated TCM and BDCM average levels (above $150 \mu\text{g L}^{-1}$) and minor DBCM concentrations ($7.17 \mu\text{g L}^{-1}$) ($n = 48$, Day>0) throughout the experiment (Fig. 3-b; Table A.3). The lme model applied to the data set from the clear mesocosms showed a significant increase (lme, $p < 0.0045$) in THMs for the intermittent treatment at Day 36 (Table A.6), which is also observable in the positive trend of the normalized THM concentration throughout the experiment for that treatment (Fig. 3-a). Despite the higher total THM levels in the clear mesocosms, TCM concentrations are higher in the brown mesocosms, reflecting its association with highly terrestrial DOM present in browning systems (Bond et al., 2012; Breider and Hunkeler, 2014).

Despite observing no significant differences in the initial formation potential of HANs between brown and clear mesocosms (see Section 3.1), the responses of HANs to the treatments in brown and clear mesocosms differed strongly (Fig. 3-c; Table A.7). DCAN was the only HAN species quantified in brown mesocosms (Fig. 3-d), and significant increases in concentration were found after daily additions on Day 20 and 36 compared to the control units (Table A.7). However, similar DCAN concentrations were observed for intermittent and extreme treatments at Day 36 (Table A.3, Table A.7). Thus, a final total HAN concentration of approximately $40 \mu\text{g L}^{-1}$ was observed for the three treatments ($n = 12$) at the end of the experiment, in contrast with the $25 \mu\text{g L}^{-1}$ of the control units ($n = 4$) (Fig. 3-d). An interesting finding from this study was the response of HANs to the different treatments in the clear mesocosms (Fig. 3-c). Although the HAN speciation was similar for all treatments during the experiment, with DCAN as the predominant specie (DCAN \gg BCAN > TCAN) (Fig. 3-d, Table A-3), the levels of these N-DBPs differed significantly for each treatment (Table A.7). The daily and intermittent additions to the clear mesocosms generated a consistent increase in HAN levels over the course of the experiment (lme, $p < 0.001$), reaching final mean concentrations of $80.15 \mu\text{g L}^{-1}$ ($n = 4$) in the case of the intermittent treatment and $59.56 \mu\text{g L}^{-1}$ ($n = 4$) for the daily treatment, in contrast to the $37.41 \mu\text{g L}^{-1}$ ($n = 3$) observed in the control units (Fig. 3-d). The response of HAN levels to extreme additions exhibited a significant increase only at Day 36 (lme, $p < 0.02$), with a mean final concentration of $41.16 \mu\text{g L}^{-1}$ ($n = 4$) (Table A.7). The dispersion of data in the DBP-FP, with high standard deviation observed in Fig. 3, reflects the combined uncertainty and variability of DBP-FP resulting from various environmental factors, mesocosm complexities and experimental procedures. This observation is not rare in mesocosm studies due to their ecological realism and increased scale (Sanderson, 2002).

3.5. Interactions between precursors and DBPs

The responses of monitored explanatory variables, encompassing both DOM composition and quantity, varied with different additions of DOM and nutrients. These responses were linked to the formation of DBPs (response variable). Throughout the experiment, 57 % of the variance in THM formation potential was explained by one PLS component while 79 % of the variance in HAN formation potential was

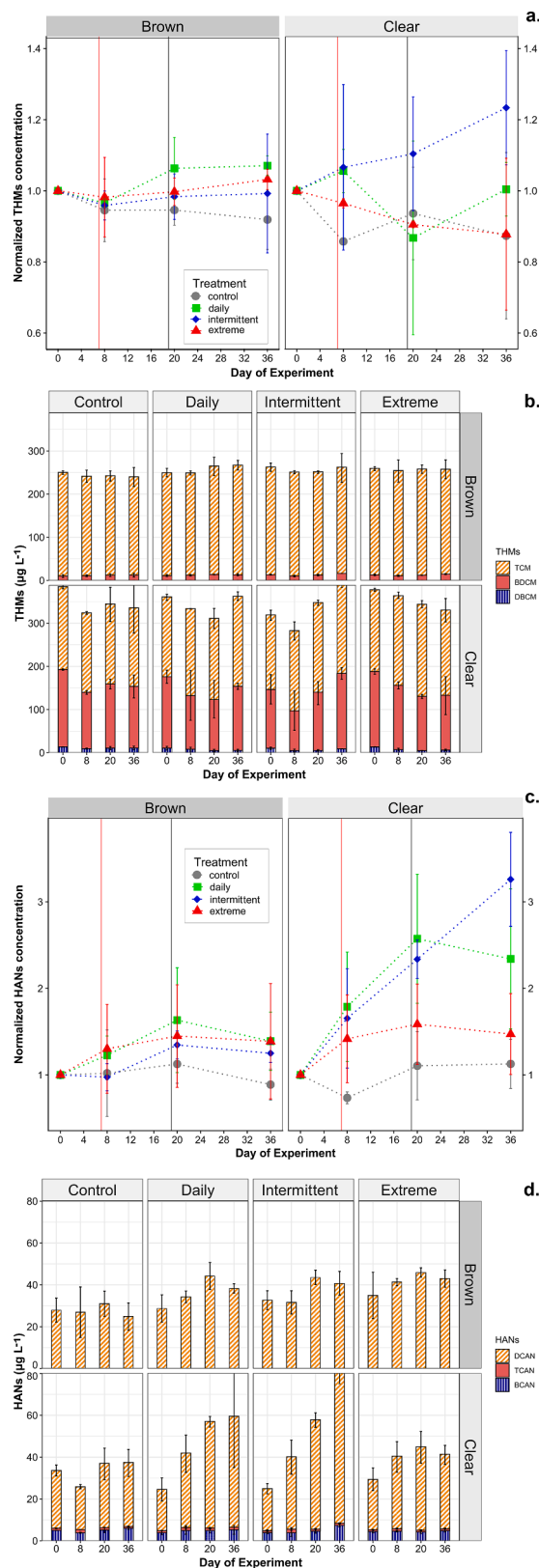


Fig. 3. DBP-FP for a. THMs and c. HANs (normalized mean concentration \pm sd, $n = 4$) measured on Days 0, 8, 20 and 36. Red vertical lines indicate when the extreme pulse took place. Gray vertical lines indicate the end of the additions period. DBP-FP species concentrations for b. THMs and d. HANs formed by treatment, by mesocosm type and by day of experiment (mean \pm sd, $n = 4$).

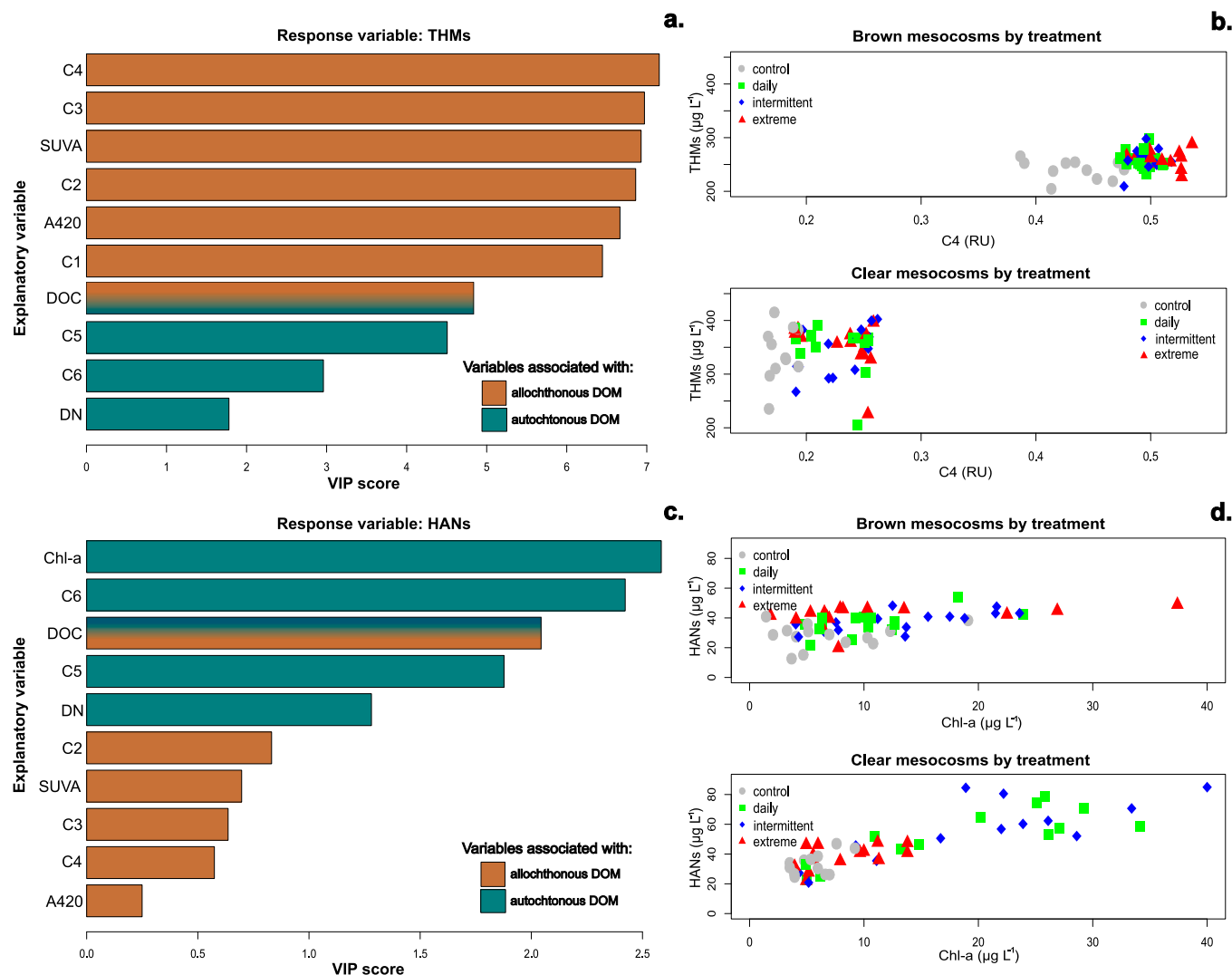


Fig. 4. Variable importance in projection (VIP) of explanatory variables for the PLS fitting models of the formation potential of a. THMs and c. HANs for all four DBP-FP sampling days. Scatter plots by treatment are shown between the most influential explanatory variable and the response variable b. THMs and d. HANs for brown and clear mesocosms.

explained by two PLS components. Identification of important explanatory variables for DBP formation was accomplished through VIP plots applied to the PLS models (Fig. 4-a, 4-c), presenting importance in descending order. All explanatory variables exhibited relatively high importance ($VIP > 1$) in THMs formation, with visible higher VIP values for variables associated with terrestrial, allochthonous DOM character (humic-like PARAFAC components, SUVA and A420) (Fig. 4-a). Conversely, only explanatory variables associated to freshly produced, autochthonous DOM (Chl-a, protein-like PARAFAC components, DN) showed notable influence ($VIP > 1$) in HANs formation (Fig. 4-c). DOC exhibited influence in both THMs and HANs formation, showing its potential as a simple DBP predictor (Peng et al., 2016). Allochthonous DOM has primarily been associated with the formation of regulated C-DBPs like THMs (Bond et al., 2012; Liao et al., 2017). However, the investigation of N-DBPs has typically occurred when chloramine is utilized as the disinfectant (Yang et al., 2015, 2010).

Further exploration of interactions between the most influential explanatory variables and DBPs formation was conducted through scatter plots considering different treatments and mesocosm types. THMs-C4 interactions exhibited diverse behaviors between mesocosm types but not among treatments (Fig. 4-b), with lower THM levels at higher C4 values in brown mesocosms and higher THM levels at lower C4 values in clear mesocosms. These observations deviate from previous

findings (Xue et al., 2014), emphasizing the potential impact of local conditions such as bromide levels and browning on the THM responses. In contrast, HANs-Chl-a interactions demonstrated positive correlations for both mesocosm types, with these relationships varying among treatments (Fig. 4-d). The noteworthy correlation observed in the clear mesocosms between HANs and Chl-a for intermittent and daily treatments suggests that the lower intensities and higher frequency of these treatments, combined with sufficient light penetration, created favorable conditions for producing HAN precursors (Hua et al., 2019; Krasner, 2009).

3.6. Implications for the drinking water sector

Regional (e.g. climate) and local (land use, land cover, hydrology) factors in a catchment collectively shape the composition of DOM and nutrients in runoff entering lakes (Doyle et al., 2019), which potentially impact the presence of DBP precursors. This study identified significant differences between two lakes, driven by local factors. For example, unexpectedly higher bromide levels in clear lake waters led to increased levels and species of THMs (Br-THMs) in clear mesocosms, emphasizing the need to monitor point and diffuse sources of bromide in catchments such as seawater intrusion (Chowdhury, 2022) and the use of deicing salts in roads (Delpla and Rodriguez, 2016). In turn, the humic

characteristics of the darker brown lake waters led to higher TCM precursors but inhibited the production of autochthonous DOM after nutrient additions, resulting in lower HAN precursors compared to the clear mesocosms. While water treatment processes including coagulation and flocculation can more effectively remove terrestrial humic-like DOM precursors (Shutova et al., 2014), the removal of protein-like DOM is more challenging, owing to its smaller size (Beggs et al., 2009), posing concerns as studies suggest higher cytotoxicity and genotoxicity for N-DBPs compared to regulated C-DBPs (Tareq Aziz et al., 2022; Xue et al., 2014). Thus, for the management of the more toxic and less regulated group of N-DBP compounds, it is relevant to consider nutrient inputs particularly in source waters used for drinking water that are clear, and especially during times of the year associated with algae blooms, which contribute directly to the production of autochthonous DOM.

Identifying and monitoring main DBP precursors in specific catchments and lakes devoted to drinking water supply can assist water managers in decision-making. For example, addressing runoff with high frequencies and low intensities through long-term responses (e.g. monitoring land-use changes and nutrient inflows to catchments), mid-term measures (e.g. controlling residence times in reservoirs to prevent eutrophication), and short-term responses (e.g., algae removal, oxidation) can mitigate the production of N-DBPs precursors. Extreme rainfall events, while showing lower DBP formation in this study, have been associated with higher C-DBPs formation, especially at the beginning of the storm. The composition of DOM entering lakes can shift over the period of a storm, and depends on antecedent soil moisture conditions (Patel et al., 2021). These high loads of precursors can stress drinking water systems in short periods, particularly in small systems with limited water source retention (e.g. reservoirs, pre-dams) or direct extraction from rivers. Hence, short-term responses are required (e.g. higher energy and chemicals dose), resulting in increased operational costs and compromised water safety when they are not planned (Anderson et al., 2023).

Climate change is likely to impact DBP precursors, highlighting two relevant events: i) Increased runoff with associated DOM and nutrients, is likely to result in higher THM precursors that could become more problematic in systems experiencing browning; and ii) High air temperatures, common during dry summer periods, can impact lake levels and inflow/outflow rates, leading to prolonged retention times and increased in-lake autochthonous DOM production. Consequently, it contributes to the production of HAN and THM precursors that could become more problematic in eutrophic ecosystems with high nutrient availability, especially in systems experiencing warmer conditions (Xiao et al., 2023). A diversity of models predicting DBP formation, especially THMs, exist in the literature (Chowdhury et al., 2009). However, using long- and short-term weather forecasts to develop tools for predicting the mobilization of DBP precursors, such as those identified in this research (e.g. DOC, Chl-a) could support water managers in addressing uncertainties arising from future climatic events and anthropogenic stressors (Lofon et al., 2023).

Given the complexity of natural processes within aquatic ecosystems, we believe that using mesocosms to study DBP precursors is a promising approach, considering factors and processes which are challenging to reproduce at the laboratory scale. A thorough characterization of the study sites and higher sampling frequency for DBP-FP tests are recommended for future studies to capture rapid responses of the aquatic ecosystems.

4. Conclusions

This study provides valuable insights into the responses of THM and HAN formation potential to runoff variability, represented by differences in timing of DOM and inorganic nutrient additions. A novel approach for DBPs studies was employed using a mesocosm experiment that was spatially and temporally coordinated in two boreal lakes,

characterized by brown (humic) and clear waters. These results are particularly relevant for the drinking water sector, especially for facilities that utilize freshwater as their source water for treatment. Key take home messages from this study include:

- Lake type (brown vs. clear waters) was the most influential factor affecting the formation potential of DBPs. Clear mesocosms exhibited higher levels of more toxic DBP precursors, driven by high bromide concentrations, which boosted the formation of Br-THMs upon disinfection. In addition, the increased light availability in the clear mesocosms enhanced the production of precursors for highly toxic and unregulated HANs.
- Runoff variability emerged as the second most influential factor impacting DBP formation potential in the clear water lake. In the clear mesocosms, intermittent and daily treatments produced higher levels of HAN and THM precursors compared to the extreme pulse. In the brown mesocosms, pulse variability led to similar levels of DBP precursors.
- Terrestrial allochthonous DOM proxies were identified as the primary drivers of THM (C-DBPs) formation potential, while fresh autochthonous DOM proxies were found to be most influential for HAN (N-DBPs) formation potential. The selection of DOM surrogates to control DBP precursors in source waters can be based on the target DBP species and/or available resources.
- Increasing uncertainty in the precipitation patterns puts safe drinking water at risk, requiring more tools to monitor and predict DBP precursors from catchments to distribution.

CRedit authorship contribution statement

Angela Pedregal-Montes: Writing – original draft, Methodology, Investigation, Formal analysis, Data curation. **Eleanor Jennings:** Writing – review & editing, Supervision, Methodology. **Dolly Kothawala:** Writing – review & editing, Methodology, Investigation, Conceptualization. **Kevin Jones:** Investigation, Data curation. **Johanna Sjøstedt:** Writing – review & editing, Resources, Formal analysis, Conceptualization. **Silke Langenheder:** Writing – review & editing, Project administration, Methodology, Investigation, Funding acquisition, Conceptualization. **Rafael Marcé:** Writing – review & editing, Supervision, Funding acquisition. **Maria José Farré:** Writing – review & editing, Supervision, Investigation.

Declaration of competing interest

The authors declare that they have no known competing financial interests or personal relationships that could have appeared to influence the work reported in this paper.

Data availability

The data used in this study is available at https://meta.fieldsites.se/collections/sggNFTTTz6C_IXghwlXaYsE1.

Acknowledgements

This project was funded by the European Union's Horizon 2020 research and innovation programme under the Marie Skłodowska-Curie grant agreement no. 956623 (MSCA-ITN-ETN-European Training Network, inventWater); the Swedish Infrastructure for Ecosystem Science (SITES), specifically the Erken Laboratory and Bolmen Research Station. SITES's current funding (2023–2028) is provided by the Swedish Research Council grant no. 2021–00164; and the Transnational Access program of the EU H2020-INFRAIA project no. 871081, AQUACOSM-plus. We thank the Technical Services of the Catalan Institute for Water Research for the analysis and quantification of DBPs, and to Lund University for supplying the Aqualog® for the DOM EEM

measurements. DK was funded by the Swedish Research Council grant no. 2020–03249. The authors express their appreciation to Stella Berger, Jens Nejstgaard, Juha Rankinen, William Colom, Nils Kreuter, Berenike Bick, Bence Buttyán, Eleni Charmpila, Jimmy Clifford Oppong, Bence Gergác, Emma Gray, Anika Happe, Congcong Jiao, Nusret Karakaya, Gabriela Ágreda López, Clara Mangold, and Katerina Symiakaki for their support and contributions to the mesocosm experimental setup and data collection. We also thank Christoffer Bergvall, Helena Enderskog, Robyn Övergaard and Margarita Judina for water chemistry analyses.

Supplementary materials

Supplementary material associated with this article can be found, in the online version, at [doi:10.1016/j.watres.2024.121791](https://doi.org/10.1016/j.watres.2024.121791).

References

- Anderson, L.E., DeMont, I., Dunnington, D.D., Bjorndahl, P., Redden, D.J., Brophy, M.J., Gagnon, G.A., 2023. A review of long-term change in surface water natural organic matter concentration in the northern hemisphere and the implications for drinking water treatment. *Sci. Total Environ.* <https://doi.org/10.1016/j.scitotenv.2022.159699>.
- APHA, 2005. AWWA and WPCF standard methods for the examination of waters and waste waters.
- Beggs, K.M.H., Summers, R.S., McKnight, D.M., 2009. Characterizing chlorine oxidation of dissolved organic matter and disinfection by-product formation with fluorescence spectroscopy and parallel factor analysis. *J. Geophys. Res. Biogeosci.* 114. <https://doi.org/10.1029/2009JG001009>.
- Bertilsson, S., Tranvik, L.J., 2000. Photochemical transformation of dissolved organic matter in lakes. *Limnol. Oceanogr.* 45, 753–762.
- Bond, T., Goslan, E.H., Parsons, S.A., Jefferson, B., 2012. A critical review of trihalomethane and haloacetic acid formation from natural organic matter surrogates. *Environmen. Technol. Rev* 1, 93–113. <https://doi.org/10.1080/09593330.2012.705895>.
- Boyle, T.P., Fairchild, J.F., 1997. The role of mesocosm studies in ecological risk analysis. *Ecolog. Applic* 7, 1099–1102. [https://doi.org/10.1890/1051-0761\(1997\)007\[1099:TROMSI\]2.0.CO;2](https://doi.org/10.1890/1051-0761(1997)007[1099:TROMSI]2.0.CO;2).
- Breider, F., Hunkeler, D., 2014. Mechanistic insights into the formation of chloroform from natural organic matter using stable carbon isotope analysis. *Geochim. Cosmochim. Acta* 125, 85–95. <https://doi.org/10.1016/j.gca.2013.09.028>.
- Burd, K., Tank, S.E., Dion, N., Quinton, W.L., Spence, C., Tanentzap, A.J., Olefeldt, D., 2018. Seasonal shifts in export of DOC and nutrients from burned and unburned peatland-rich catchments, Northwest Territories, Canada. *Hydrol. Earth. Syst. Sci.* 22, 4455–4472. <https://doi.org/10.5194/hess-22-4455-2018>.
- Calderó-Pascual, M., Yıldız, D., Yalçın, G., Metin, M., Yetim, S., Fiorentin, C., Andersen, M.R., Jennings, E., Jeppesen, E., Ger, K.A., Beklioglu, M., McCarthy, V., 2021. The importance of allochthonous organic matter quality when investigating pulse disturbance events in freshwater lakes: a mesocosm experiment. *Hydrobiologia.* <https://doi.org/10.1007/s10750-021-04757-w>.
- Chang, C.J., Huang, C.P., Chen, C.Y., Wang, G.S., 2020. Assessing the potential effect of extreme weather on water quality and disinfection by-product formation using laboratory simulation. *Water Res* 170. <https://doi.org/10.1016/j.watres.2019.115296>.
- Chen, C., Zhang, X.jian, Zhu, L.xia, Liu, J., He, W.jie, Han, H.da, 2008. Disinfection by-products and their precursors in a water treatment plant in North China: seasonal changes and fraction analysis. *Sci. Total Environ* 397, 140–147. <https://doi.org/10.1016/j.scitotenv.2008.02.032>.
- Chowdhury, S., 2022. Effects of seawater intrusion on the formation of disinfection byproducts in drinking water. *Sci. Total Environ* 827.
- Chowdhury, S., Champagne, P., McLellan, P.J., 2009. Models for predicting disinfection byproduct (DBP) formation in drinking waters: a chronological review. *Sci. Total Environ.* <https://doi.org/10.1016/j.scitotenv.2009.04.006>.
- Clarke, K.R., 1993. Non-parametric multivariate analyses of changes in community structure. *Austral. J. Ecol* 18, 117–143. <https://doi.org/10.1111/j.1442-9993.1993.tb00438.x>.
- Clutterbuck, B., Yallop, A.R., 2010. Land management as a factor controlling dissolved organic carbon release from upland peat soils 2: changes in DOC productivity over four decades. *Sci. Total Environ* 408, 6179–6191. <https://doi.org/10.1016/j.scitotenv.2010.08.038>.
- Coble, P.G., Green, S.A., Blough, N.V., Gagosian, R.B., 1990. Characterization of dissolved organic matter in the Black Sea by fluorescence spectroscopy. *Nature* 432, 432–435.
- Criquet, J., Rodriguez, E.M., Allard, S., Wellauer, S., Salhi, E., Joll, C.A., von Gunten, U., 2015. Reaction of bromine and chlorine with phenolic compounds and natural organic matter extracts - electrophilic aromatic substitution and oxidation. *Water Res* 85, 476–486. <https://doi.org/10.1016/j.watres.2015.08.051>.
- Dejaeger, K., Criquet, J., Billon, G., 2022. Identification of disinfection by-product precursors by natural organic matter fractionation: a review. <https://doi.org/10.21203/rs.3.rs-1660564/v1>.
- Delpla, I., Jung, A.V., Baures, E., Clement, M., Thomas, O., 2009. Impacts of climate change on surface water quality in relation to drinking water production. *Environ. Int.* <https://doi.org/10.1016/j.envint.2009.07.001>.
- Delpla, I., Rodriguez, M.J., 2016. Experimental disinfection by-product formation potential following rainfall events. *Water Res* 104, 340–348. <https://doi.org/10.1016/j.watres.2016.08.031>.
- Doyle, B.C., De Eyto, E., Dillane, M., Poole, R., McCarthy, V., Ryder, E., Jennings, E., 2019. Synchrony in catchment stream colour levels is driven by both local and regional climate. *Biogeosciences* 16, 1053–1071. <https://doi.org/10.5194/bg-16-1053-2019>.
- Eder, A., Weigelhofer, G., Pucher, M., Tiefenbacher, A., Strauss, P., Brandl, M., Blöschl, G., 2022. Pathways and composition of dissolved organic carbon in a small agricultural catchment during base flow conditions. *Ecohydrol. Hydrobiol* 22, 96–112. <https://doi.org/10.1016/j.ecohyd.2021.07.012>.
- Erken Laboratory, 2023. Meteorological data from Erken, Malma island, 1988-10-13 - 2022-12-30. Swed. Infrastruc. Ecosyst. Sci. (SITES).
- Evlampidou, I., Font-Ribera, L., Rojas-Rueda, D., Gracia-Lavedan, E., Costet, N., Pearce, N., Vineis, P., Jaakkola, J.J.K., Delloye, F., Makris, K.C., Stephanou, E.G., Kargaki, S., Kozisek, F., Sigsgaard, T., Hansen, B., Schullehner, J., Nahkur, R., Galey, C., Zwiener, C., Vargha, M., Righi, E., Aggazzotti, G., Kalnina, G., Grazuleviciene, R., Polanska, K., Gubkova, D., Bitenc, K., Goslan, E.H., Kogevinas, M., Villanueva, C.M., 2020. Trihalomethanes in drinking water and bladder cancer burden in the European Union. *Environ. Health Perspect* 128. <https://doi.org/10.1289/EHP4495>.
- Farré, M.J., Jaén-Gil, A., Hawkes, J., Petrovic, M., Catalán, N., 2019. Orbitrap molecular fingerprint of dissolved organic matter in natural waters and its relationship with NDMA formation potential. *Sci. Total Environ* 670, 1019–1027. <https://doi.org/10.1016/j.scitotenv.2019.03.280>.
- Favilla, S., Durante, C., Vigni, M.L., Cocchi, M., 2013. Assessing feature relevance in NPLS models by VIP. *Chemom. Intell. Labor. Syst* 129, 76–86. <https://doi.org/10.1016/j.chemolab.2013.05.013>.
- Fellman, J.B., Hood, E., Spencer, R.G.M., 2010. Fluorescence spectroscopy opens new windows into dissolved organic matter dynamics in freshwater ecosystems: a review. *Limnol. Oceanogr.* <https://doi.org/10.4319/lo.2010.55.6.2452>.
- Feuchtmayr, H., Pottinger, T.G., Moore, A., De Ville, M.M., Cailouet, L., Carter, H.T., Pereira, B.M., Maberly, S.C., 2019. Effects of brownification and warming on algal blooms, metabolism and higher trophic levels in productive shallow lake mesocosms. *Sci. Total Environ* 678, 227–238. <https://doi.org/10.1016/j.scitotenv.2019.04.105>.
- Fonseca, B.M., Levi, E.E., Jensen, L.W., Graeber, D., Søndergaard, M., Lauridsen, T.L., Jeppesen, E., Davidson, T.A., 2022. Effects of DOC addition from different sources on phytoplankton community in a temperate eutrophic lake: an experimental study exploring lake compartments. *Sci. Total Environ* 803. <https://doi.org/10.1016/j.scitotenv.2021.150049>.
- Golea, D.M., Upton, A., Jarvis, P., Moore, G., Sutherland, S., Parsons, S.A., Judd, S.J., 2017. THM and HAA formation from NOM in raw and treated surface waters. *Water Res* 112, 226–235. <https://doi.org/10.1016/j.watres.2017.01.051>.
- Heeb, M.B., Criquet, J., Zimmermann-Steffens, S.G., Von Gunten, U., 2014. Oxidative treatment of bromide-containing waters: formation of bromine and its reactions with inorganic and organic compounds - a critical review. *Water Res* 48, 15–42. <https://doi.org/10.1016/j.watres.2013.08.030>.
- Hua, G., Reckhow, D.A., Abusallout, I., 2015. Correlation between SUVA and DBP formation during chlorination and chloramination of NOM fractions from different sources. *Chemosphere* 130, 82–89. <https://doi.org/10.1016/j.chemosphere.2015.03.039>.
- Hua, G., Reckhow, D.A., Kim, J., 2006. Effect of bromide and iodide ions on the formation and speciation of disinfection byproducts during chlorination. *Environ. Sci. Technol* 40, 3050–3056. <https://doi.org/10.1021/es0519278>.
- Hua, L.C., Lai, C.H., Wang, G.S., Lin, T.F., Huang, C., 2019. Algogenic organic matter derived DBPs: precursor characterization, formation, and future perspectives—a review. *Crit. Rev. Environ. Sci. Technol* 49, 1803–1834. <https://doi.org/10.1080/10643389.2019.1586057>.
- Jennings, E., Eyto, E.de, Moore, T., Dillane, M., Ryder, E., Allott, N., Aonghusa, C.N., Rouen, M., Poole, R., Pierson, D.C., 2020. From highs to lows: changes in dissolved organic carbon in a peatland catchment and lake following extreme flow events. *Water (Switzerland)* 12. <https://doi.org/10.3390/w12102843>.
- Jentsch, A., Kreyling, J., Beierkuhnlein, C., 2007. A new generation of climate-change experiments: events, not trends. *Front. Ecol. Environ* 5 (7), 365–374.
- Karlsson, J., Byström, P., Ask, J., Ask, P., Persson, L., Jansson, M., 2009. Light limitation of nutrient-poor lake ecosystems. *Nature* 460, 506–509. <https://doi.org/10.1038/nature08179>.
- Komaki, Y., Ibuki, Y., 2022. Inhibition of nucleotide excision repair and damage response signaling by dibromoacetonitrile: a novel genotoxicity mechanism of a water disinfection byproduct. *J. Hazard. Mater* 423. <https://doi.org/10.1016/j.jhazmat.2021.127194>.
- Kothawala, D.N., Ji, X., Laudon, H., Ågren, A.M., Futter, M.N., Köhler, S.J., Tranvik, L.J., 2015. The relative influence of land cover, hydrology, and in-stream processing on the composition of dissolved organic matter in boreal streams. *J. Geophys. Res. Biogeosci* 120, 1491–1505. <https://doi.org/10.1002/2015JG002946>.
- Kothawala, D.N., Murphy, K.R., Stedmon, C.A., Weyhenmeyer, G.A., Tranvik, L.J., 2013. Inner filter correction of dissolved organic matter fluorescence. *Limnol. Oceanogr. Methods* 11, 616–630. <https://doi.org/10.4319/lom.2013.11.616>.
- Kothawala, D.N., Stedmon, C.A., Müller, R.A., Weyhenmeyer, G.A., Köhler, S.J., Tranvik, L.J., 2014. Controls of dissolved organic matter quality: evidence from a large-scale boreal lake survey. *Glob. Chang. Biol* 20, 1101–1114. <https://doi.org/10.1111/gcb.12488>.

- Krasner, S.W., 2009. The formation and control of emerging disinfection by-products of health concern. *Mathemat., Phys. Engineer. Sci.* <https://doi.org/10.1098/rsta.2009.0108>.
- Kumar, K., Margerum, D.W., 1987. Kinetics and mechanism of general-acid-assisted oxidation of bromide by hypochlorite and hypochlorous acid. *Inorg. Chem.*
- Langenheder, S., Kreuter, N., Sassenhagen, I., Berger, S., Kothawala, D., Mesman, J., Nejstgaard, J., Striebel, M., Sjöstedt, J., Karakaya, N., 2024. SITES AquaNet - AQUACOSM-plus run off variability experiment. <https://doi.org/10.23700/KKFA-HY54>.
- Lavonen, E., 2015. Tracking Changes in Dissolved Natural Organic Matter composition : Evaluating Drinking Water Production Using Optical and Molecular Level Tools. Swedish University of Agricultural Sciences, Uppsala.
- Lawaetz, A.J., Stedmon, C.A., 2009. Fluorescence intensity calibration using the raman scatter peak of water. *Appl. Spectrosc.* 63, 936–940.
- Ledesma, J.L.J., Köhler, S.J., Futter, M.N., 2012. Long-term dynamics of dissolved organic carbon: implications for drinking water supply. *Sci. Total Environ.* 432, 1–11. <https://doi.org/10.1016/j.scitotenv.2012.05.071>.
- Lee, Y., Von Gunten, U., 2009. Transformation of 17 β -ethinylestradiol during water chlorination: effects of bromide on kinetics, products, and transformation pathways. *Environ. Sci. Technol.* 43, 480–487. <https://doi.org/10.1021/es8023989>.
- Leenheer, J., Croué, J.-P., 2003. Peer reviewed: characterizing aquatic dissolved organic matter. *Environ. Sci. Technol.* 37 (1), 18A–26A.
- Leenheer, J.A., 2009. Systematic approaches to comprehensive analyses of natural organic matter. *Annal. Environmen. Sci.* 3. Retrieved from. <https://openjournals.neu.edu/aes/journal/article/view/3art1>.
- Li, X.F., Mitch, W.A., 2018. Drinking water disinfection byproducts (DBPs) and human health effects: multidisciplinary challenges and opportunities. *Environ. Sci. Technol.* 52, 1681–1689. <https://doi.org/10.1021/acs.est.7b05440>.
- Liao, X., Chen, C., Yuan, B., Wang, J., Zhang, X., 2017. Control of nitrosamines, THMS and HAAs in heavily impacted water with O3-BAC. *Amer. Water Works Assoc.* 109, E215–E225. <https://doi.org/10.5942/jawwa.2017.109.0057>.
- Lipczynska-Kochany, E., 2018. Effect of climate change on humic substances and associated impacts on the quality of surface water and groundwater: a review. *Sci. Total Environ.* <https://doi.org/10.1016/j.scitotenv.2018.05.376>.
- Liu, P., Farré, M.J., Keller, J., Gernjak, W., 2016. Reducing natural organic matter and disinfection by-product precursors by alternating oxic and anoxic conditions during engineered short residence time riverbank filtration: a laboratory-scale column study. *Sci. Total Environ.* 565, 616–625. <https://doi.org/10.1016/j.scitotenv.2016.05.061>.
- Lofton, M.E., Howard, D.W., Thomas, R.Q., Carey, C.C., 2023. Progress and opportunities in advancing near-term forecasting of freshwater quality. *Glob. Chang. Biol.* 29, 1691–1714. <https://doi.org/10.1111/gcb.16590>.
- Monteith, D.T., Stoddard, J.L., Evans, C.D., De Wit, H.A., Forsius, M., Högåsen, T., Wilander, A., Skjelkvåle, B.L., Jeffries, D.S., Vuorenmaa, J., Keller, B., Kopéček, J., Veselý, J., 2007. Dissolved organic carbon trends resulting from changes in atmospheric deposition chemistry. *Nature* 450, 537–540. <https://doi.org/10.1038/nature06316>.
- Munthali, E., Marcé, R., Farré, M.J., 2022. Drivers of variability in disinfection by-product formation potential in a chain of thermally stratified drinking water reservoirs. *Environ. Sci. (Camb)* 8, 968–980. <https://doi.org/10.1039/d1ew00788b>.
- Murphy, K.R., Stedmon, C.A., Graeber, D., Bro, R., 2013. Fluorescence spectroscopy and multi-way techniques. *PARAFAC. Analyt. Methods.* <https://doi.org/10.1039/c3ay41160e>.
- Murphy, K.R., Stedmon, C.A., Wenig, P., Bro, R., 2014. OpenFluor- An online spectral library of auto-fluorescence by organic compounds in the environment. *Analyt. Methods* 6, 658–661. <https://doi.org/10.1039/c3ay41935e>.
- Myhre, G., Alterskjær, K., Stjern, C.W., Hodnebrog, Marelle, L., Samset, B.H., Sillmann, J., Schaller, N., Fischer, E., Schulz, M., Stohl, A., 2019. Frequency of extreme precipitation increases extensively with event rareness under global warming. *Sci. Rep.* 9. <https://doi.org/10.1038/s41598-019-52277-4>.
- Parlanti, E., Woë Rz, K., Geoffroy, L., Lamotte, M., 2000. Dissolved organic matter fluorescence spectroscopy as a tool to estimate biological activity in a coastal zone submitted to anthropogenic inputs. *Org. Geochem.* 31, 1765–1781.
- Patel, K.F., Myers-Pigg, A., Bond-Lamberty, B., Fansler, S.J., Norris, C.G., McKeever, S.A., Zheng, J., Rod, K.A., Bailey, V.L., 2021. Soil carbon dynamics during drying vs. rewetting: importance of antecedent moisture conditions. *Soil. Biol. Biochem.* <https://doi.org/10.1016/j.soilbio.2021.108165>.
- Peleato, N.M., Andrews, R.C., 2015. Comparison of three-dimensional fluorescence analysis methods for predicting formation of trihalomethanes and haloacetic acids. *J. Environ. Sci. (China)* 27, 159–167. <https://doi.org/10.1016/j.jes.2014.04.014>.
- Peng, D., Saravia, F., Abbt-Braun, G., Horn, H., 2016. Occurrence and simulation of trihalomethanes in swimming pool water: a simple prediction method based on DOC and mass balance. *Water Res.* 88, 634–642. <https://doi.org/10.1016/j.watres.2015.10.061>.
- Pilla, R.M., Griffiths, N.A., 2023. Integrating reservoirs into the dissolved organic matter versus primary production paradigm: how does chlorophyll-a change across dissolved organic carbon concentrations in reservoirs? *Ecosystems.* <https://doi.org/10.1007/s10021-023-0087>.
- R. Core Team, 2023. R: a language and environment for statistical computing.
- Richardson, S.D., 2011. Disinfection by-products: formation and occurrence in drinking water. in: *Encyclopedia Og Environmental Health.* pp. 110–136. <https://doi.org/10.1016/B978-0-444-52272-6.00276-2>.
- Richardson, S.D., 2003. Disinfection by-products and other emerging contaminants in drinking water. *TrAC* 22, 666–684. [https://doi.org/10.1016/S0165-9936\(03\)01003-3](https://doi.org/10.1016/S0165-9936(03)01003-3).
- Riedel, T., Biester, H., Dittmar, T., 2012. Molecular fractionation of dissolved organic matter with metal salts. *Environ. Sci. Technol.* 46, 4419–4426. <https://doi.org/10.1021/es203901u>.
- Sanchís, J., Jaén-Gil, A., Gago-Ferrero, P., Munthali, E., Farré, M.J., 2020. Characterization of organic matter by HRMS in surface waters: effects of chlorination on molecular fingerprints and correlation with DBP formation potential. *Water Res.* 176. <https://doi.org/10.1016/j.watres.2020.115743>.
- Sanderson, H., 2002. Pesticide Studies: replicability of micro/mesocosms. *Environmental. Sci. & Pollut. Res.* 9, 429–435. <https://doi.org/10.1007/BF02987597>.
- Shutova, Y., Baker, A., Bridgeman, J., Henderson, R.K., 2014. Spectroscopic characterisation of dissolved organic matter changes in drinking water treatment: from PARAFAC analysis to online monitoring wavelengths. *Water Res.* 54, 159–169. <https://doi.org/10.1016/j.watres.2014.01.053>.
- Soulié, T., Stibor, H., Mas, S., Braun, B., Knechtel, J., Nejstgaard, J.C., Sommer, U., Vidussi, F., Mostajir, B., 2022. Brownification reduces oxygen gross primary production and community respiration and changes the phytoplankton community composition: an in situ mesocosm experiment with high-frequency sensor measurements in a North Atlantic bay. *Limnol. Oceanogr.* 67, 874–887. <https://doi.org/10.1002/lno.12041>.
- Stedmon, C.A., Bro, R., 2008. Characterizing dissolved organic matter fluorescence with parallel factor analysis: a tutorial. *Limnol. Oceanogr. Methods* 6, 572–579.
- Stewart, R.L.A., Dossena, M., Bohan, D.A., Jeppesen, E., Kordas, R.L., Ledger, M.E., Meerhoff, M., Moss, B., Mulder, C., Shurin, J.B., Suttle, B., Thompson, R., Trimmer, M., Woodward, G., 2013. Mesocosm experiments as a tool for ecological climate-change research. *Advances in Ecological Research* 71–181. <https://doi.org/10.1016/B978-0-12-417199-2.00002-1>.
- Tak, S., Vellanki, B.P., 2018. Natural organic matter as precursor to disinfection byproducts and its removal using conventional and advanced processes: state of the art review. *J. Water Health* 16, 681–703. <https://doi.org/10.2166/wh.2018.032>.
- Tareq Aziz, M., Granger, C.O., Westerman, D.C., Putnam, S.P., Ferry, J.L., Richardson, S.D., 2022. Microseira wollei and Phormidium Algae more than doubles DBP concentrations and calculated toxicity in drinking water.
- Urrutia-Cordero, P., Langvall, O., Blomkvist, P., Angeler, D.G., Bertilsson, S., Colom Montero, W., Eklöv, P., Aagaard Jakobsen, N., Klemetsson, L., Laudon, H., Liljebadh, B., Lundgren, M., Parkefeld, L., Kelpsiene, E., Pierson, D., Rankinen, J., Striebel, M., Tranvik, L.J., Weslien, P., Hillebrand, H., Langenheder, S., 2021. SITES AquaNet: an open infrastructure for mesocosm experiments with high frequency sensor monitoring across lakes. *Limnol. Oceanogr. Methods* 19, 385–400. <https://doi.org/10.1002/lom3.10432>.
- Uzun, H., Zhang, W., Olivares, C.I., Erdem, C.U., Coates, T.A., Karanfil, T., Chow, A.T., 2020. Effect of prescribed fires on the export of dissolved organic matter, precursors of disinfection by-products, and water treatability. *Water Res.* 187. <https://doi.org/10.1016/j.watres.2020.116385>.
- Valdivia-García, M., Weir, P., Graham, D.W., Werner, D., 2019. Predicted impact of climate change on trihalomethanes formation in drinking water treatment. *Sci. Rep.* 9. <https://doi.org/10.1038/s41598-019-46238-0>.
- Wang, D., Chen, Y., Jarin, M., Xie, X., 2022. Increasingly frequent extreme weather events urge the development of point-of-use water treatment systems. *NPJ. Clean. Water* 5. <https://doi.org/10.1038/s41545-022-00182-1>.
- Wang, X., Zhang, H., Zhang, Y., Shi, Q., Wang, J., Yu, J., Yang, M., 2017. New insights into Trihalomethane and Haloacetic Acid formation potentials: correlation with the molecular composition of natural organic matter in source water. *Environ. Sci. Technol.* 51, 2015–2021. <https://doi.org/10.1021/acs.est.6b04817>.
- Wang, X.X., Liu, B.M., Lu, M.F., Li, Y.P., Jiang, Y.Y., Zhao, M.X., Huang, Z.X., Pan, Y., Miao, H.F., Ruan, W.Q., 2021. Characterization of algal organic matter as precursors for haloacetic and nitrogenous disinfection byproducts formation: comparison with natural organic matter. *J. Environ. Manage.* 282. <https://doi.org/10.1016/j.jenvman.2021.111951>.
- Wawryk, N.J.P., Craven, C.B., Blackstock, L.K.J., Li, X.F., 2021. New methods for identification of disinfection byproducts of toxicological relevance: progress and future directions. *J. Environ. Sci. (China)*. <https://doi.org/10.1016/j.jes.2020.06.020>.
- Wei, X., Yang, M., Zhu, Q., Wagner, E.D., Plewa, M.J., 2020. Comparative Quantitative Toxicology and QSAR Modeling of the Haloacetonitriles: forcing Agents of Water Disinfection Byproduct Toxicity. *Environ. Sci. Technol.* 54, 8909–8918. <https://doi.org/10.1021/acs.est.0c02035>.
- Weyhenmeyer, G.A., Müller, R.A., Norman, M., Tranvik, L.J., 2016. Sensitivity of freshwaters to browning in response to future climate change. *Clim. Change* 134, 225–239. <https://doi.org/10.1007/s10584-015-1514-z>.
- Williams, C.J., Conrad, D., Kothawala, D.N., Baulch, H.M., 2019. Selective removal of dissolved organic matter affects the production and speciation of disinfection byproducts. *Sci. Total Environ.* 652, 75–84. <https://doi.org/10.1016/j.scitotenv.2018.10.184>.
- Xiao, R., Deng, Y., Xu, Z., Chu, W., 2023. Disinfection byproducts and their precursors in drinking water sources: origins, influencing factors, and environmental insights. *Engineering.* <https://doi.org/10.1016/j.eng.2023.08.017>.
- Xu, J., Morris, P.J., Liu, J., Ledesma, J.L.J., Holden, J., 2020. Increased dissolved organic carbon concentrations in peat-fed UK water supplies under future climate and sulfate deposition scenarios. *Water Resour. Res.* 56. <https://doi.org/10.1029/2019WR025592>.
- Xue, C., Wang, Q., Chu, W., Templeton, M.R., 2014. The impact of changes in source water quality on trihalomethane and haloacetonitrile formation in chlorinated drinking water. *Chemosphere* 117, 251–255. <https://doi.org/10.1016/j.chemosphere.2014.06.083>.

- Yang, L., Kim, D., Uzun, H., Karanfil, T., Hur, J., 2015. Assessing trihalomethanes (THMs) and N-nitrosodimethylamine (NDMA) formation potentials in drinking water treatment plants using fluorescence spectroscopy and parallel factor analysis. *Chemosphere* 121, 84–91. <https://doi.org/10.1016/j.chemosphere.2014.11.033>.
- Yang, X., Fan, C., Shang, C., Zhao, Q., 2010. Nitrogenous disinfection byproducts formation and nitrogen origin exploration during chloramination of nitrogenous organic compounds. *Water Res* 44, 2691–2702. <https://doi.org/10.1016/j.watres.2010.01.029>.
- Yang, X., Shang, C., Lee, W., Westerhoff, P., Fan, C., 2008. Correlations between organic matter properties and DBP formation during chloramination. *Water Res* 42, 2329–2339. <https://doi.org/10.1016/j.watres.2007.12.021>.